# Nuclear structure and band mixing in $^{194}$Pt

A. Jalili Majarshin,[1] Yan-An Luo,[1] Feng Pan,[2,4] H. T. Fortune,[3] and Jerry P. Draayer[4]

[1]*School of Physics, Nankai University, Tianjin 300071, P.R. China*

[2]*Department of Physics, Liaoning Normal University, Dalian 116029, P.R. China*

[3]*Department of Physics and Astronomy, University of Pennsylvania, Philadelphia, Pennsylvania 19104, USA*

[4]*Department of Physics and Astronomy, Louisiana State University, Baton Rouge, Louisiana 70803-4001, USA*

(Received 16 October 2020; revised 17 December 2020; accepted 22 January 2021; published 16 February 2021)

We introduce a two-particle, two-hole mixed configuration scheme to fit $E2$ strengths for the $0 \leftrightarrow 2$, $2 \leftrightarrow 4$, and $4 \leftrightarrow 6$ transitions in $^{194}$Pt. The interaction includes two sets of pairing operators, $\{S^{\pm}(t), S^{0}(t)\}$ $(t = s, d)$. Solutions within this framework are used to analyze energy spectra, $E2$ transitions, and band-mixing features of the model. The results confirm that mixing is small and similar for $J = 2$, 4, and 6, with the calculated energies and transition matrix elements in excellent agreement with experimental data.

DOI: 10.1103/PhysRevC.103.024317

## I. INTRODUCTION

Nuclear structure studies that include band mixing at low energies have attracted much attention from both experimental and theoretical perspectives. In this regard, one of the more successful models is the interacting boson model (IBM) [1–4]. Specifically, within the IBM framework one finds strong evidence for band mixing [4–7] involving multi-particle-hole excitations [2,8]. From a theoretical perspective, a commonly used model for investigating quantum phase transitions is the IBM [1], with three dynamical symmetries, namely, a vibrational [U(5)] mode, a $\gamma$-soft [O(6)] mode, and a rotational [SU(3)] mode [9–12]. One can consider band mixing configurations due to multi-particle-hole excitations, which is confirmed to be useful in describing intruder states near closed-shell nuclei, typically those around proton numbers $Z \sim 50$ and $Z \sim 82$ [2,8].

Accordingly, numerous configurations with roughly the same excitation energies can exist [1,6,13,14]. More precisely, the lowest-lying $0^+$ and $2^+$ states can become strongly mixed such that it is very tricky to allocate a configuration label to them. Recently, configuration mixing in the O(6) and U(5) limits were proposed [15,16]. We have offered and developed SU(1,1) coherent states to describe band mixing [15,16]. Fortune in Refs. [17–21] has described the band mixing between the ground and excited states of $K = 0$ and/or $K = 2$ bands in $^{72}$Ge, $^{74-78}$Kr, $^{106,108}$Pd, $^{154}$Gd, and $^{182,184}$Hg. Likewise, there are many publications involving the band-mixed configurations in medium and heavy mass nuclei [15,16,22]. It is not uncommon to find partial energy spectra and transition rates that are consistent with one or more configuration mixing schemes.

The existence of shape coexistence phenomena is associated with particle-hole (np-nh) excitations across the shell closure. It has been shown that IBM with higher-order interactions is a highly successful phenomenological model in the description of both collective valence shell and multi-particle-hole excitations in nuclei for which there is clear evidence for the presence of mixing of particle-hole configurations and eventual mixing of two coexisting collective states. Various workers have estimated the mechanism of the $J^{\pi} = 0^+, 2^+, 4^+, 6^+$ ($K = 0^+$ bands) and $J^{\pi} = 2^+, 3^+, 4^+, \ldots$ ($K = 2^+$ bands) ground-gamma or gamma-beta band-mixing. Coexistence and mixing between $K = 0^+$ and $K = 2^+$ bands can be prevalent at low energy [23–26]. The configuration mixing scheme based on the multi-particle-hole excitations is common in understanding shape coexistence configuration and nuclear structure by taking different symmetry limits of the IBM. Several regions are of great interest with different shapes. When passing from light to heavy isotopes, the Pt region is characterized by variation from the U(5)-SU(3) axis to the $\gamma$-soft U(5)-O(6) axis [27–30]. It is a widely acknowledged interpretation that $^{194}$Pt involves coexistence and mixing. Providing two approaches U(5)-O(6) and $\gamma$-soft rotor Hamiltonians to explain coexisting structures and shape changes, the question is which is most appropriate to $^{194}$Pt. Nuclear structure in Pt isotopes, including triaxiality, has been studied with $\gamma$ softness playing a prominent role. The nuclear structure in $^{194}$Pt can be understood in terms of various observables. The selected observables to be analyzed herein are energies and $E2$ transitions. In our previous work [22], we presented an exact solution of the U(5)-O(6) transitional description in the IBM with two-particle and two-hole configuration mixing based on the Bethe ansatz formalism to determine the normal and intruder states and $E2$ transition rates. In the present paper, we report the assignment of additional information, such as band mixing, not presented in our previous publication [22].

In nuclear structure theory, it is very important to get the energy spectra and transition rates correct. Here, we employ a relatively simple solvable pairing model that includes two-particle and two-hole configuration mixing based on the affine SU(1,1) Lie algebra [31–34]. The associated Hamiltonian we

 

use generates two-particle, two-hole mixing to calculate partial low-lying level energies and $B(E2)$ rates. It is within this framework that we show this configuration mixing scheme is an effective model for systematically exploring band mixing in ground and excited states. The main goals of this study involve two aspects. First, to find shape coexistence or quantum phase transitions based on a simplified configuration-mixing scheme. Second, it is demonstrated that the simple two-state model seems necessary to describe the band mixing in $^{194}$Pt. It is further shown that deformation can be well described by quadrupole-quadrupole interaction in the standard coherent state of the IBM-1. Using the $\gamma$-soft rotor Hamiltonian, we can describe the deformation based on coherent state configuration.

## II. CALCULATIONS AND RESULTS

Here, we present the pairing Hamiltonian of configuration mixing scheme for transitional nuclei. References [15,16,22] are the best reviews of studies with the configuration mixing scheme. Also, we make use of quasi-spin algebras, which have been explained in detail in Refs. [31,34,35]. By using this relation as generators of SU(1,1) algebra for $\rho = s$ and $d$ boson we have $S^+(\rho) = \frac{1}{2}\rho^\dagger.\rho^\dagger$ for creation operator of bosons, $S^-(\rho) = \frac{1}{2}\tilde{\rho}.\tilde{\rho}$ for annihilation operator and $S^0(\rho) = \frac{1}{2}(\rho^\dagger.\tilde{\rho} + \frac{2\rho+1}{2})$ for number-conserving operator with $\rho = 0$ for $s$ boson and $\rho = 2$ for $d$ boson [31].

We use the theory of affine SU(1,1) algebraic technique [31], which determines the properties of energy spectra, mixing of states, and electric transition rates. By employing the generators of SU(1,1) algebra in terms of $\rho$-boson operators, the solvable Hamiltonian is constructed for the transitional region between normal U(5) and the intruder O(6) configurations. The Hamiltonian can be written as $\hat{H} = S_0^+ S_0^- + S_\rho^0$ by adding the second Casimir operator, where $\rho^\dagger$ is the creation operator of $\rho$ bosons and $\tilde{\rho}_\nu = (-1)^\nu \rho_{-\nu}$.

The Hamiltonian, which describes the interaction between the normal and deformed bands, is formed by two-boson creation and annihilation with 2p2h excitations. For the sake of band mixing, we have the combination of two terms in the Hamiltonian as $H = H_{\rm IBM} + H_{\rm Mix}$. So the Hamiltonian to describe the band mixing may be written as [15,16]

$$\hat{H} = P_N\big(\hat{H}^{(1)}_{\rm IBM}\big)\, P_N + P_{N+2}\big(\hat{H}^{(2)}_{\rm IBM}\big)\, P_{N+2} + P(\hat{H}_{\rm Mix})\, P, \quad (1)$$

where $P_N$ and $P$ are projection operators, which projects to the $N$-boson subspace, while $P$ project to the subspace with $N$ and $N+2$ bosons,

$$\hat{H}^{(i)}_{\rm IBM} = a_s^{(i)} S_s^0 + a_d^{(i)} S_d^0 + g^{(i)} S^+ S^-, \quad (2)$$

for $i = 1$ and 2 are the U(5)-O(6) transitional Hamiltonians [31], and for two-configuration mixing we have

$$\begin{aligned}\hat{H}_{\rm Mix} &= g_s(s^\dagger \times s^\dagger + s \times s) + g_d(d^\dagger \times d^\dagger + \tilde{d} \times \tilde{d}) \\ &= g_s(S_s^+ + S_s^-) + g_d(S_d^+ + S_d^-). \end{aligned} \quad (3)$$

We have the SU(1,1) algebra, which satisfies the commutation relations

$$\big[S^0_{\rho'}, S^\pm_\rho\big] = \pm\delta_{\rho'\rho} S^\pm_\rho, \quad [S^+_{\rho'}, S^-_\rho] = -2\delta_{\rho'\rho} S^0_\rho. \quad (4)$$

Basis vectors $|N; \tau\, \nu_s \nu_d \eta L M\rangle$ can also be expressed as those SU(1,1) algebra with two sets of operators $\{S^\pm_\rho, S^0_\rho\}$ for $d$ and $s$ bosons,

$$|N, \tau\, \nu_s \nu_d \eta L M\rangle = (-1)^\tau N (S_s^+)^{\frac{N-\nu_d-\nu_s}{2}-\tau} (S_d^+)^\tau |\nu_s; \nu_d \eta L M\rangle, \quad (5)$$

in which $n_d = 2\tau + \nu_d$ and $\tau = 0, 1, 2, \ldots, \frac{1}{2}(N - \nu_d - \nu_s)$ with $\nu_s = 0$, 1. Here $N$, $v$, $L$ are the total number of bosons, seniority numbers, and angular momentum quantum number, respectively, with the third component of the angular momentum $M$. To distinguish different states with the same $L$, we need an additional quantum number $\eta$.

To get the Bethe ansatz approach, the eigenstate of Eq. (1) can be written as

$$\begin{aligned}&|\tau\, \nu_s; \nu_d \eta L M\rangle \\ &= \left(\alpha^\tau_{\nu_s,\nu_d,\eta,L} \prod_{\rho=1}^{k} S^+\big(x_\rho^{(\tau)}\big) + \beta^\tau_{\nu_s,\nu_d,\eta,L} \prod_{\rho=1}^{k+1} S^+\big(y_\rho^{(\tau)}\big)\right) \\ &\quad \times |\nu_s; \nu_d \eta L M\rangle, \end{aligned} \quad (6)$$

where $\alpha_{\nu_s,\nu_d,\eta,L}$ and $\beta_{\nu_s,\nu_d,\eta,L}$, in general, are complex numbers to be determined, $\tau$ labels the $\tau$th set of the solution $(x_1^\tau, \ldots x_k^\tau, y_1^\tau, \ldots y_{k+1}^\tau)$ with the $k$ numbers of pairing. The explicit form of the functional $S^+(x)$ is similar to the format used in Ref. [35],

$$S^+(x) = xS^+(s) + S^+(d), \quad (7)$$

where $x$ is the spectral parameter to be determined. Gaudin first introduced an equivalent form of $S^+(x)$ as an ansatz in determining the exact solutions of a spin-spin interaction scheme [36], which is now applied to be a consistent operator form in designing the Bethe ansatz wave-function Eq. (6) for the configuration mixing scheme in IBM. By using the commutation relation and act of Hamiltonian to the Bethe ansatz wave-function Eq. (6) and diagonalization, $\hat{H}|\tau\, \nu_s; \nu_d \eta L M\rangle = E^\tau_{\nu_s,\nu_d,L}|\tau\, \nu_s; \nu_d \eta L M\rangle$, we can get the eigenvalues similar to the form used in Ref. [35].

It has been shown that the Platinum isotopes are suitable candidates within the U(5)-O(6) transitional area. As illustrated in the earlier study [30,37], the vibrational feature in $^{172-194}$Pt isotopes is not insignificant, mainly in $A \leqslant 190$. U(5) and O(6) limits are pertinent to the normal and intruder states, respectively [38,39]. It means that Pt isotopes as collective nuclei with multiphonon excitations of particle-hole configuration lead us to the shape coexistence between normal U(5) and intruder SO(6) configuration. For this reason, however, the existence of intruder states in $^{182-184}$Pt isotopes is much more obvious, so that the present model based on the configuration mixing scheme is only appropriate to explain $^{194}$Pt, which is closest to the O(6)-limit in the Casten triangle [30,37]. Using the band mixing Hamiltonian Eq. (1) with Bethe Ansatz approach, we can explain most aspects of the ground and excited states of $^{194}$Pt up to 2.5 MeV. The Bethe Ansatz approach has been explained in detail in Refs. [15,16,22]. Energy spectra can be constructed based on the diagonalization in the $N \oplus (N+2)$-boson subspace, of which the complete basis vectors in each configuration

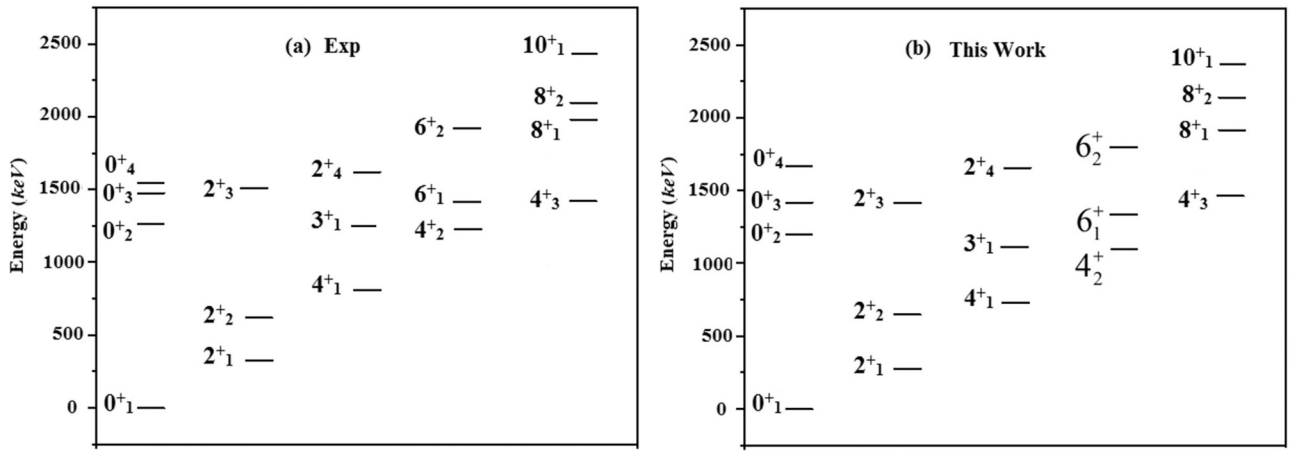


FIG. 1. Some low-lying energy levels for (a) experimental and (b) theoretical result in $^{194}$Pt. Available experimental data were taken from Ref. [40].

can be taken as those of U(6)⊃ U(5)⊃ O(5)⊃ O(3) with $|N, \nu_s\nu_d\eta LM\rangle$. In the diagonalization, the Hamiltonian Eq. (1) is applied to obtain a low-lying spectrum of $^{194}$Pt with $N = 2\tau + \nu_s + \nu_d$, for which the term $\hat{H}_L = L.L$ is added to Eq. (1) to lift the degeneracy of the levels with the same seniority to form the angular momentum sequences with different angular momentum quantum numbers. One note to mention is that in the Hamiltonian, if $g^{(1)} = g^{(2)} = 0$, the system is in the O(6)-limit without configuration mixing. With the variation of $g$ values, the mixing occurs. Energy spectra of low-lying states related to band mixing in $^{194}$Pt are plotted and compared in Fig. 1.

The model parameters are taken as $a_s^{(1)} = 0$, $a_d^{(1)} = 1.05$ MeV, $g^{(1)} = -1$ keV, $a_s^{(2)} = 150$ keV, $a_d^{(2)} = 1.17$ MeV, $g^{(2)} = -72$ keV, $g_s = 200$ keV, and, $g_d = 150$ keV. It can be observed that the ground and some partial excited states below 2.5 MeV, which belong to the band mixing, are included. Moreover, the energy spectra with odd-spin and parity assignments ($J^-$) are also not included. In addition, some excited states higher than 2.42 MeV, such as $7^+_1$, $10^+_2$, and so on, are not considered due to the pair-broken state with major components of proton-holes in $1h_{11/2}$-orbit and neutron-holes in $i_{13/2}$-orbit. Also, We have plotted energies versus $J(J+1)$ for band 1, 2, $k = 2$ and other in Fig. 2. Theoretical calculations can be verified against the experimental energy spectra shown in Ref. [40] that most ground and excited states are fitted quite well. The root-mean-square deviation, $\sigma = 174.89$keV is calculated between the calculated energy spectra and experimental counterparts.

Only levels of normal states with ($N = 2\tau + \nu_d + \nu_d$, $\nu \leqslant 3$), and intruder levels are shown in the figures. In Fig. 1 we see that the first set of levels with $\tau = 1$ are the same as those generated from the model without configuration mixing ($g = 0$), the second set of levels with $\tau = 2$ are built on the intruder $0^+_4$ level to the normal ground level, and so on. Each set of the levels with $\tau \geqslant 2$ is a reproduction of those with $\tau = 1$ generated from the original intruder O(6) limit. Also, we know from Fig. 2 that all the known positive-parity states below 1.65 MeV are plotted, but only high-$J$ above that energy. Two tentative ($5^+$) states are included. Band 1 is the ground band, band 2 is the beginning of a band based on the excited $0^+$ state. Placements of states within bands were guided by energies and $E2$ strengths. Both the energy and $E2$ behavior indicate that the second $2^+$ state is not associated with the second $0^+$ state. That distinction belongs to the third or fourth $2^+$. All other states below 1.65 MeV are indicated as "other." Odd-$J$ states with positive parity are placed in the $K = 2$ band.

Excited states with leading $J^\pi = 2^+, 3^+, 4^+$ ($K = 2^+$ bands) components are allocated to the $\gamma$ band, while the $\beta$ band includes states defined by dominant $J^\pi = 0^+, 2^+, 4^+, 6^+$ ($K = 0^+$ bands) components. The mixing configuration calculation reproduces the experimental values, in particular, it predicts that the first excited band-head $0^+_2$ has the lowest excitation energy in quasi-$\beta$ band groups with respect to $\beta$ deformation, while the first excited band-head $2^+_2$ has the lowest excitation energy in quasi-$\gamma$ band groups. Excited energies are also in quantitative agreement with experimental data. It must be pointed out that the $0^+_2$, $2^+_3$, and $4^+_3$ levels are allocated to the quasi-$\beta$ bands. Similarly, as one can see in Fig. 1, the calculated $3^+_1$ and the $4^+_2$ levels in $^{194}$Pt are allocated to the quasi-$\gamma$ bands lying on top of the $2^+_2$ state.

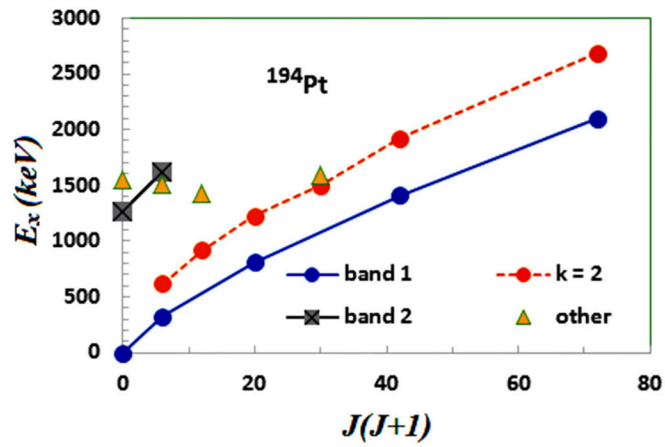


FIG. 2. Plot of excitation energy vs. $J(J+1)$ for first three bands in $^{194}$Pt.

In the next step by the simple model, we have a mixing of the states ($K = 0^+$ bands) and ($K = 2^+$ bands), assigned to the ground and $\gamma$ bands, respectively.

Pairing model with a configuration mixing scheme is applied to describe the energy spectra and $E2$ transition rates in which the configuration mixing scheme keeps the lower part of the $\gamma$-unstable spectrum unchanged and generates the intruder states through the mixing term. Describing the shape coexistence pattern can be achieved by mixing the normal U(5) and the intruder O(6) configurations. The observed intruder states in even-even Pt isotopes are well-known in the Casten triangle [28,41,42]. Their presence in even-even nuclei can be explained with an intruder O(6)-limit Hamiltonian. Also, there are still many experimental signatures [27,43] revealing the presence of $\gamma$-soft O(6) nuclei in Pt isotopes. That's why we have selected the O(6)-limit Hamiltonian in our work. We should also consider that Pt isotopes with configuration mixing exist in a region of the nuclear chart, around the proton shell closure $Z = 82$, characterized by different deformations [44]. Furthermore, the O(6) quadrupole-quadrupole interaction in connection with the shape coexistence phenomenon within a coherent state requires the presence of states with very different deformations. One might try to use this property to establish a coherent theory of triaxiality in the IBM framework. It is proved [45] that the coherent state procedure is acceptable between quantum parameters and geometrical parameters. The classical equilibrium shapes and their evolution of a nucleus described by IBM have been studied [46,47] to show the potential shape of Eq. (8) in the classical limit. The most general Hamiltonian is of the form

$$\hat{H}_O = \zeta \hat{Q}.\hat{Q} + \xi \hat{L}^2 + \phi T_3 + \chi T_4, \tag{8}$$

where $\zeta, \xi, \phi,$ and $\chi$ are adjustable parameters and $T_3 = \frac{\sqrt{30}}{6}(\hat{L} \times \hat{Q} \times \hat{L})^{(0)}$ and $T_4 = -\frac{5\sqrt{3}}{18}[(\hat{L} \times \hat{Q})^{(1)} \times (\hat{L} \times \hat{Q})^{(1)}]^{(0)}$ are the operators with quadrupole-quadrupole interaction terms. To obtain a more intuitive insight into the problem of triaxial shapes and validate our work, we use the standard coherent state defined as [48]

$$|N, \beta, \gamma\rangle = [N!(1+\beta^2)^N]^{-(1/2)}(s^\dagger + \beta\cos\gamma d_0^\dagger + \frac{1}{\sqrt{2}}\beta\sin\gamma(d_2^\dagger + d_{-2}^\dagger)^N|0\rangle. \tag{9}$$

As it can be seen, there are quasi-$\beta$ and quasi-$\gamma$ bands from the ground band up to $8_1^+$. The authors of Ref. [30] investigated the Pt isotopes in the IBM framework by using the extended consistent-$Q$ framework, in which intruder configuration was not taken into account. It has been shown in Refs. [30,37], that some partial energy spectra below 1.5 MeV in $^{194}$Pt were included. It can be said that the energy of $5_1^+$ state in both the IBM and the extended consistent-$Q$ framework displayed in Ref. [37] is 0.5–0.7 MeV higher than the corresponding experimental value. Actually, there are $4^+, 5^+, 6^+$, and $8^+$ states with excitation energy ~2.0 MeV. One could assume that the energy spectra of other excited states with higher angular momentum quantum numbers provided from both the IBM and the extended consistent-$Q$ framework calculations would also be much higher than the corresponding experimental values. Now we can get the expectation value in the coherent state with $\langle N, \beta, \gamma|\hat{H}_O|N, \beta, \gamma\rangle$ in Fig. 3.

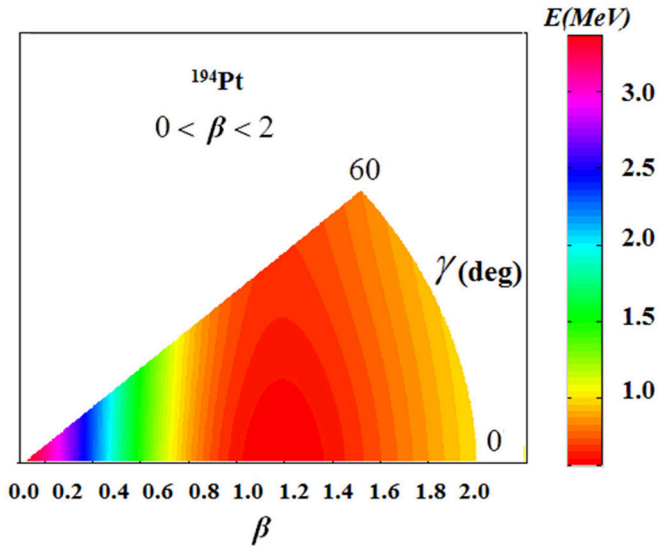


FIG. 3. The potential-energy surface in $^{194}$Pt. The expectation value in the coherent state used with the configuration mixing calculations. We observe that the parameter $\chi$ taken to be 0 is always better as far as the level energies are concerned. The other parameters used are $\zeta = -3.3$ keV, $\xi = 2.8$ keV, and $\phi = -3.5$ keV, for the $0_2^+$ level energy.

When we are moved higher than the critical area, the minimal region becomes a global minimum point around $\beta = 1.4$ and $\gamma = 60$ (deg), indicating that an oblate phase appears. In addition, $\gamma$ varies from 0 to 60 in the equilibrium valley at the critical area, which indicates a $\gamma$-soft shape [1].

Based on the above points, let us turn to the band mixing in some ground and excited states. The existence of intruder states leads to the band mixing, which is unavoidable, especially to explain the $B(E2)$ values. Also, a simple two-state model can work well when we have intruder states involved in the band mixing. Typically, band mixings are associated with the normal ground and excited intruder states. The simple two-state model has been used to describe the band mixing in connection with the intruder states. At this point, it is worthwhile to determine the band mixing in $^{194}$Pt. It has been found that coexistence configurations is described by mixing between the normal U(5) and the intruder O(6) configuration in Pt isotope. On the other hand, this configuration can make a condition where the normal configuration approaches the U(5) limit while the intruder configuration is closer to the O(6) limit. Suppose the normal states (N bosons) with vibration limit and the intruder states (N+2 bosons) with rotational limit coexist, they can interact and mix. In that case, the total lowest weight $|lw\rangle$ wave function can be $A|lw_N\rangle_{(g)} + B|lw_{N+2}\rangle_{(e)}$, where the subscripts $g$ and $e$ refer to the ground and excited bands, respectively, and $|lw\rangle \equiv N, n_d, \nu, n_\Delta, L, M$.

If all the matrix elements $M(E2)$ are known, then the mixing analysis for $0 \leftrightarrow 2$, $2 \leftrightarrow 4$, and $4 \leftrightarrow 6$, for example, can be done separately. Here, we could not apply the band

mixing for $0 \leftrightarrow 2$. It doesn't apply in the present case because the second $2^+$ state is not connected to the second $0^+$ state. We have applied the simple two-state mixing to the transitions $2 \leftrightarrow 4$ and $4 \leftrightarrow 6$.

We introduce two bands as the Refs. [17–21], $g$ and $e$, with $2^+$, $4^+$, and $6^+$ basis-state wave functions $2_g$, $2_e$; $4_g$, $4_e$; and $6_g$, $6_e$, respectively. We have

$$|lw\rangle_{(2_1^+)}(^{194}\mathrm{Pt}) = A|lw\rangle_{(g)} + B|lw\rangle_{(e)},$$
$$|lw\rangle_{(2_2^+)}(^{194}\mathrm{Pt}) = B|lw\rangle_{(g)} - A|lw\rangle_{(e)}, \quad (10)$$

for $2_1^+$ and $2_2^+$ states,

$$|lw\rangle_{(4_1^+)}(^{194}\mathrm{Pt}) = C|lw\rangle_{(g)} + D|lw\rangle_{(e)},$$
$$|lw\rangle_{(4_2^+)}(^{194}\mathrm{Pt}) = D|lw\rangle_{(g)} - C|lw\rangle_{(e)}, \quad (11)$$

for $4_1^+$ and $4_2^+$ or higher states, and

$$|lw\rangle_{(6_1^+)}(^{194}\mathrm{Pt}) = E|lw\rangle_{(g)} + F|lw\rangle_{(e)},$$
$$|lw\rangle_{(6_2^+)}(^{194}\mathrm{Pt}) = F|lw\rangle_{(g)} - E|lw\rangle_{(e)}, \quad (12)$$

for $6_1^+$ and $6_2^+$ or higher states, where the coefficients of $A$, $B$, $C$, $D$, $E$, and $F$ are the mixing amplitudes.

There is a unique determination for the two-state model based on the Refs. [17–21]. But here we develop an exact solution based on the configuration mixing scheme. Details about exact solutions have been presented in Refs. [15,16,22,31]. For various multi-particle-hole configurations, we need the effective boson charge to calculate the $E2$ transitions [8,13,14,49]. The $E2$ operator is written as

$$T_\mu^{(E2)} = q_{e2}\hat{P}_N\left[(s^\dagger \times \tilde{d} + d^\dagger \times \tilde{s})_\mu^{(2)}\right]\hat{P}_N + q'_{e2}\hat{P}\left[(s^\dagger \times \tilde{d} + d^\dagger \times \tilde{s})_\mu^{(2)}\right]\hat{P}, \quad (13)$$

where $\hat{P}_N$ is the projection operator onto the configuration mixing without multiparticle-hole excitations. And $B(E2)$ is given by

$$B(E2; \alpha_i L_i \to \alpha_f L_f) = \frac{|\langle \alpha_f L_f || T^{E2} || \alpha_i L_i \rangle|^2}{2L_i + 1}, \quad (14)$$

where the reduced matrix element is defined in terms of the Clebsch-Gordan coefficients and $\langle \alpha_f L_f || \hat{I} || \alpha_i L_i \rangle = \delta_{\alpha_f,\alpha_i}\delta_{L_f,L_i}$ with unit identity operator $\hat{I}$.

For projection operator we have

$$\hat{P}|N', n_d, \nu, n_\Delta, L, M\rangle = \begin{cases} |N', n_d, \nu, n_\Delta, L, M\rangle & \text{if } N' \geqslant N \\ 0 & \text{otherwise} \end{cases}, \quad (15)$$

which keeps the operator effective only within the boson subspace by $[N] \oplus [N+2] \oplus [N+4] \oplus \ldots$ mixed configurations. As those shown in Refs. [15,16], the band mixing from the ground up to the excited states in the normal and intruder bands $2^+$, $4^+$, and $6^+$ of $^{194}$Pt deduced in Ref. [40] are considered. The best global fit produces the model parameters for $E2$ transitions to the experimental data. The fitted partial $B(E2)$ transitions are shown in Fig. 4, in which the corresponding results of the $2n$-particle and $2n$-hole configuration mixing are also provided. The reduced matrix elements of $T(E2)$ based on the configuration mixing obtained in this work agree to the corresponding experimental results.

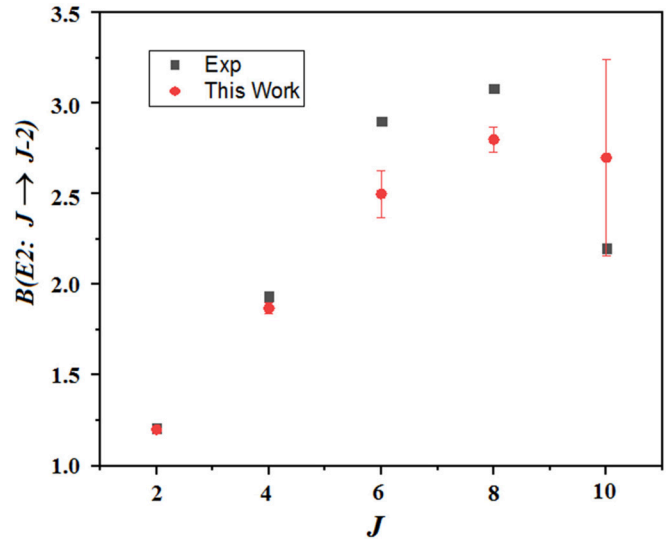


FIG. 4. E2 transition rates for lowest $J \to J\text{-}2$ transitions in $^{194}$Pt. Available experimental data with error bars were taken from Ref. [40].

Furthermore, most transition matrix elements calculated in this work agree with the experimental data. Each value is very close to the corresponding result calculated from the configuration mixing scheme. Based on the experimental $E2$ transition matrix elements, for the $M_0$ label, we have 0.749 eb, and for the $M_1$ label, we have 0.0069 eb. So, $B(E2, 2_1^+ \to 4_1^+)$ is 108 times larger than $B(E2, 2_2^+ \to 4_1^+)$, furthermore $B(E2, 6_1^+ \to 4_1^+)$ is 18 times larger than the corresponding experimental value of $B(E2, 4_2^+ \to 6_1^+)$. Similar to the $B$ $(E2;\ J_i \to J_f)$ result we have the same pattern for $M$ $(E2;\ J_i \to J_f)$ results.

Here, we define the matrix elements $M_g$ and $M_e$ for connecting $2^+$ and $4^+$ states and also $M'_g$ and $M'_e$ for connecting $4^+$ and $6^+$ states

$$M_g = \langle 2_g | E2 | 4_g \rangle, \quad M_e = \langle 2_e | E2 | 4_e \rangle, \quad (16)$$

TABLE I. $E2$ transition matrix elements ($eb$) for $0 \leftrightarrow 2$ transitions in $^{194}$Pt.

| Label | $i$ | $f$ | $M(E2)$ Exp.[a] | $M(E2)$ This work |
|---|---|---|---|---|
| $M_0$ | $2_1^+$ | $0_1^+$ | 2.45 | 2.73 |
| $M_1$ | $2_2^+$ | $0_1^+$ | 0.66 | 0.89 |
| $M_2$ | $2_3^+$ | $0_2^+$ | Unknown | 1.70 |
| $M_3$ | $2_3^+$ | $0_1^+$ | Unknown | 0.93 |
| $M_4$ | $0_2^+$ | $2_1^+$ | 0.26 | 0.29 |
| $M_5$ | $0_2^+$ | $2_2^+$ | 0.48 | 0.88 |
| $M_6$ | $0_4^+$ | $2_1^+$ | 0.55 | 0.60 |
| $M_7$ | $0_4^+$ | $2_2^+$ | 0.55 | 0.26 |

[a]Used $M(E2)$ from Ref. [51].

TABLE II. $E2$ strengths and transition matrix elements for $2 \leftrightarrow 4$ transitions in $^{194}$Pt.

| | | | $B(E2)(e^2b^2)$ | $M(E2)(eb)$ | | |
|---|---|---|---|---|---|---|
| Label | $i$ | $f$ | Exp.[a] | Exp. | C Exp.[b] | This work |
| $M0$ | $2_1^+$ | $4_1^+$ | $0.749^{+0.016}_{-0.010}$ | $1.935^{+0.021}_{-0.013}$ | $1.935^{+0.021}_{-0.013}$ | 1.935 |
| $M1$ | $2_2^+$ | $4_1^+$ | $0.0069^{+0.0100}_{-0.0029}$ | $0.186^{+0.135}_{-0.039}$ | $0.25^{+0.14}_{-0.06}$ | 0.0 |
| $M2$ | $2_1^+$ | $4_2^+$ | 0.0027(4) | 0.116(9) | 0.220(9) | 0.11 |
| $M3$ | $2_2^+$ | $4_2^+$ | 0.26(5) | 1.14(11) | $1.784^{+0.045}_{-0.029}$ | 1.43 |

[a]Used $M(E2)$ from Ref. [50].
[b]from Ref. [51].

and

$$M'_g = \langle 4_g|E2|6_g\rangle, \quad M'_e = \langle 4_e|E2|6_e\rangle. \tag{17}$$

Furthermore, we assume that for the band mixing of the ground and excited states, the $g$ states are not connected to the $e$ states by the $E2$ operator. We select eight transitions, connecting $0 \leftrightarrow 2$ from $M_0 - M_7$ in Table I.

Experimental result of $\sum_{i=0}^{7} M_i^2$, connecting $0 \leftrightarrow 2$ from $M_0 - M_7$, is 7.33 $e^2b^2$. The theoretical result of $\sum_{i=0}^{7} M_i^2$ without considering unknown transitions, connecting $0 \leftrightarrow 2$ from $M_0 - M_7$, is 9.51 $e^2b^2$. We have similar magnitudes for $\sum_i M_i^2$ connecting $2 \leftrightarrow 4$ and $4 \leftrightarrow 6$. Here, $M$ $(E2;\ J_i \rightarrow J_f)$, is defined as $M^{\,2}(E2;\ J_i \rightarrow J_f\ ) = (2J_i + 1)$ $B(E2;\ J_i \rightarrow J_f)$.

Also, We select eight transitions, including the four $E2$ transitions, connecting $2 \leftrightarrow 4$ from $M0 - M3$, and four $E2$ transitions, connecting $4 \leftrightarrow 6$ from $M'0 - M'3$ in $^{194}$Pt. These transition matrix elements are listed in Tables II and III.

Based on the experimental data and pairing model, the corresponding results obtained from the configuration mixing scheme for the $2 \leftrightarrow 4$ and $4 \leftrightarrow 6$ fits are shown in Tables IV and V for comparison in $^{194}$Pt.

Good agreement between experiment and model is obvious from the $M$'s. Based on the fitting for experimental data and model calculations, we have compared the ratios of basis-state matrix elements in Table VI.

Mixing is found to be small and similar for $J = 2$, 4, and 6 by the fitting values of wave-function amplitudes. For $M_g$, $M_e$, $M'_g$, and $M'_e$, it is shown that $M'_g > M_g$ and $M'_e > M_e$. The ratios $M'_g/M_g$ and $M'_e/M_e$ are larger than both the rotational and vibrational limits. Also we have seen that the experimental $B$ $(E2;\ 6_1 \rightarrow 4_1)$ is larger than the value from the pairing model calculation. These patterns are the same as Refs. [17–21] in the band mixing.

TABLE III. $E2$ transition matrix elements for $4 \leftrightarrow 6$ transitions in $^{194}$Pt from Coulomb excitation.

| | | | $M(E2)$ | $M(E2)$ |
|---|---|---|---|---|
| Label | $i$ | $f$ | C Exp.[a] | This work |
| $M'0$ | $6_1^+$ | $4_1^+$ | $2.90^{+0.10}_{-0.04}$ | 2.310 |
| $M'1$ | $4_2^+$ | $6_1^+$ | $0.16^{+0.06}_{-0.16}$ | 0.0 |
| $M'2$ | $6_1^+$ | $4_2^+$ | $0.224^{+0.017}_{-0.019}$ | 0.217 |
| $M'3$ | $6_2^+$ | $4_2^+$ | $2.09^{+0.11}_{-0.07}$ | 1.87 |

[a]Used $M(E2)$ from Ref. [51].

We have obtained some partial transition matrix elements for mixing band by fitting procedure. Transition matrix elements for $M$ $(E2;\ 2_1^+ \rightarrow 4_1^+)$ and $M'$ $(E2;\ 6_1^+ \rightarrow 4_1^+)$ have very strong strength for $2 \leftrightarrow 4$ and $4 \leftrightarrow 6$. Based on the Coulomb excitation data, the value of $M$ $(E2;\ 2_1^+ \rightarrow 4_1^+)$ is 7.74 times larger than the value of $M$ $(E2;\ 2_2^+ \rightarrow 4_1^+)$, while, the value of $M'$ $(E2;\ 6_1^+ \rightarrow 4_1^+)$ is 18.12 times larger than the value of $M'$ $(E2;\ 4_2^+ \rightarrow 6_1^+)$ in configuration mixing scheme. It means that the lower basis-state band is slightly more collective than the excited states. Of course, the $4^+$ mixing in the $2 \leftrightarrow 4$ and $4 \leftrightarrow 6$ analyses should be the same. Usually, the two results are not exactly equal, but usually, they can be made to be equal by making minor changes in one or more of the M's. In the present case, $D$ from Fit 2 is nowhere near $D$ from the $4 \leftrightarrow 6$ fit. For Fit 1, the value of $D$ is quite close to the value from the $4 \leftrightarrow 6$ analysis, and equality is easily achieved by a minor adjustment to any of the input matrix elements. This demonstrates that Fit 2 is invalid. The large difference between the two experimental values of $M3$ [50,51] remains a minor mystery, but the present analysis indicates a strong preference for the smaller value.

For particular evidence and justification, the experimental sum of $M^2$ and $M'^2$ for connecting $2 \leftrightarrow 4$ and $4 \leftrightarrow 6$ is proportional to the sum of configuration mixing model. The experimental sum of transition matrix elements, $M^2$ and $M'^2$, for connecting $2 \leftrightarrow 4$ and $4 \leftrightarrow 6$ is 4.99 and 12.85 $(e^2b^2)$, respectively. In contrast, the theoretical sum of transition matrix elements, $M^2$ and $M'^2$, for connecting $2 \leftrightarrow 4$ and $4 \leftrightarrow 6$ is 5.79 and 8.96 $(e^2b^2)$, respectively. The theoretical calculations are somewhat less collective than the experimental sum of

TABLE IV. Results of fitting $2 \leftrightarrow 4$ and $4 \leftrightarrow 6$ matrix elements in $^{194}$Pt.

| $2 \leftrightarrow 4$ | | | $4 \leftrightarrow 6$ | |
|---|---|---|---|---|
| | Fit (1)[a] | Fit (2)[b] | | |
| Quantity | Value | Value | Quantity | Value |
| $B$ | 0.191 | 0.540 | $D$ | 0.213 |
| $D$ | 0.169 | 0.523 | $F$ | 0.226 |
| $M_g(eb)$ | 1.96 | 2.03 | $M'_g$ | 2.94 |
| $M_e(eb)$ | 1.07 | 1.69 | $M'_e$ | 2.05 |

[a]Used $M3 = 1.14(11)\,eb$ obtained by combining $4_2^+$ lifetime and branching ratio [50].
[b]Used $M3 = 1.784^{+0.045}_{-0.029} eb$ from Coulomb excitation [51].

TABLE V. Results of fitting pairing model $2 \leftrightarrow 4$ and $4 \leftrightarrow 6$ matrix elements in $^{194}$Pt.

| $2 \leftrightarrow 4$ | | | $4 \leftrightarrow 6$ | |
|---|---|---|---|---|
| | Fit (1)[a] | Fit (2)[b] | | |
| Quantity | Value | Value | Quantity | Value |
| $B$ | 0.091 | 0.201 | $D$ | 0.202 |
| $D$ | 0.123 | 0.202 | $F$ | 0.252 |
| $M_g(eb)$ | 1.94 | 1.96 | $M'_g$ | 2.34 |
| $M_e(eb)$ | 1.42 | 1.41 | $M'_e$ | 1.85 |

[a]Using results from last column of Tables II.
[b]Using $M_1 = 0.107eb$, rather than 0, to get agreement for $D$.

transition matrix elements. Of course, in the two-state mixing procedure, the sums of $M^2$ and $M'^2$ are conserved

In the extraction procedure for results of fitting experimental, $2 \leftrightarrow 4$ transitions, the values of transition matrix elements for the $g$ and $e$ band are about 1.96 and 1.07 $eb$, with a ratio of 1.83. Moreover, we have the same procedure for connecting the $4 \leftrightarrow 6$ transitions. The values of transition matrix elements for the $g$ and $e$ band are about 2.94 and 2.05 $eb$, with a ratio of 1.43. Results of fitting in pairing model calculation, connecting the $2 \leftrightarrow 4$ transitions, the values of transition matrix elements for the $g$ and $e$ band are about 1.94 and 1.42 $eb$, with a ratio of 1.36. For connecting the $4 \leftrightarrow 6$ transitions, the values of transition matrix elements in pairing model calculation for the $g$ and $e$ band are about 2.34 and 1.85 $eb$, with a ratio of 1.26. Recent studies have shown the interesting results for the $R = M_e/M_g$ and $R' = M'_e/M'_g$ ratios. The ratio of transition matrix elements for connecting $2 \leftrightarrow 4$ is compatible to the $4 \leftrightarrow 6$ transitions in our model. Our results suggest that basis-state transition matrix elements for $g$ bands are stronger than $e$ bands.

We have shown energy levels and relevant transition matrix elements from the fits for the pairing model with a configuration mixing scheme. A detailed similarity of most of the ground excited states up to 2.5 MeV with known electric quadrupole transition rates obtained in this work to the experimental results [40,51] have been presented in the figures. It can be found from figures and tables that the explanations of the band mixing for connecting the $2 \leftrightarrow 4$ and $4 \leftrightarrow 6$ transitions in $^{194}$Pt values are quite excellent. Not only the energy spectra and even the transition rates, but also the positions of the ground and excited states of $2^+$, $4^+$, and $6^+$ are correctly reproduced, indicating that a lower basis-state is somewhat more collective than the second one. Finally, exact solution of the vibrational to $\gamma$-soft transitional region proposed in this work may also be valuable in diagonalizing a more comprehensive pattern dependent consistent-Q formalism in the same configuration mixing scheme, though only a solvable procedure is possible in even-even $^{172-196}$Pt, which will be considered in our future work.

TABLE VI. Ratios of $(6 \rightarrow 4)/(4 \rightarrow 2)$ basis-state matrix elements from fitting and from various models.

| Ratio | Fit to Exp. | Model ratio | Fit to Model Calcs. |
|---|---|---|---|
| $M'_g/M'_g$ | 1.5 | – | 1.2 |
| $M'_e/M'_e$ | 1.9 | – | 1.3 |
| Vibrational | – | 1.47 | – |
| Rotational $K = 2$ | – | 1.69 | – |
| Rotational $K = 0$ | – | 1.26 | – |

## III. SUMMARY AND CONCLUSION

This work explains energy spectra and transition rates of $\gamma$-soft nuclei such as $^{194}$Pt. A solvable model in transitional Hamiltonian of the interacting boson model with two-particle and two-hole configuration mixing is proposed. By adding the configuration mixing Hamiltonian ($H_{\rm mix}$) in pairing model, we have achieved the band mixing in the ground and excited states. Diagonalization method was made with configuration mixing scheme, which is designed for energy spectra and electric quadrupole transition rates. Configuration mixing scheme has been applied to members of some lowest ground and excited states of $2^+$, $4^+$, and $6^+$ bands in $^{194}$Pt. Results indicate that the lower basis-state band is slightly more collective than the excited-state band.

## ACKNOWLEDGMENTS

Support from the National Natural Science Foundation of China (Grants No. 11875171, No. 11675071, No. 11747318), the US National Science Foundation (Grants No. OIA-1738287 and No. ACI -1713690), the US Department of Energy (Grant No. DE-SC0005248), the Southeastern Universities Research Association, the China–US Theory Institute for Physics with Exotic Nuclei (CUSTIPEN) (Grant No. DE-SC0009971), and the LSU–LNNU joint research program (9961) is acknowledged.

[1] F. Iachello and A. Arima, *The Interacting Boson Model* (Cambridge University Press, Cambridge, UK, 1987).
[2] J. Wood, K. Heyde, W. Nazarewicz, M. Huyse, and P. Van Duppen, Phys. Rep. **215**, 101 (1992).
[3] R. Julin, K. Helariutta, and M. Muikku, J. Phys. G: Nucl. Part. Phys. **27**, R109 (2001).
[4] J.-E. García-Ramos and K. Heyde, Phys. Rev. C **100**, 044315 (2019).
[5] V. Hellemans, R. Fossion, S. D. Baerdemacker, and K. Heyde, Phys. Rev. C **71**, 034308 (2005).
[6] A. Frank, P. Van Isacker, and C. E. Vargas, Phys. Rev. C **69**, 034323 (2004).
[7] M. Bender, P.-H. Heenen, and P.-G. Reinhard, Rev. Mod. Phys. **75**, 121 (2003).
[8] K. Heyde and J. L. Wood, Rev. Mod. Phys. **83**, 1655 (2011).
[9] D. Rowe, Nucl. Phys. A **745**, 47 (2004).
[10] C. E. Alonso, J. M. Arias, L. Fortunato, and A. Vitturi, Phys. Rev. C **72**, 061302(R) (2005).
[11] J. M. Arias, J. E. García-Ramos, and J. Dukelsky, Phys. Rev. Lett. **93**, 212501 (2004).

[12] R. Bijker and A. Frank, Phys. Rev. C **62**, 014303 (2000).
[13] P. D. Duval and B. R. Barrett, Phys. Lett. B **100**, 223 (1981).
[14] P. D. Duval and B. R. Barrett, Nucl. Phys. A **376**, 213 (1982).
[15] F. Pan, D. Li, G. Cheng, Z. Qiao, J. Bai, and J. P. Draayer, Phys. Rev. C **97**, 034316 (2018).
[16] F. Pan, S. Yuan, Z. Qiao, J. Bai, Y. Zhang, and J. P. Draayer, Phys. Rev. C **97**, 034326 (2018).
[17] H. T. Fortune, Phys. Rev. C **95**, 044317 (2017).
[18] H. T. Fortune, Eur. Phys. J. A **54**, 178 (2018).
[19] H. T. Fortune, Eur. Phys. J. A **54**, 229 (2018).
[20] H. T. Fortune, Phys. Rev. C **98**, 064303 (2018).
[21] H. T. Fortune, Phys. Rev. C **100**, 044303 (2019).
[22] L. Dai, F. Pan, Z. Feng, Y. Zhang, S. Cui, and J. Draayer, Chin. Phys. C **44**, 064102 (2020).
[23] D. Bonatsos, Phys. Lett. B **200**, 1 (1988).
[24] N. Minkov *et al.*, Phys. Rev. C **61**, 064301 (2000).
[25] Berghe, G. Vanden, H. E. De Meyer, and P. Van Isacker, Phys. Rev. C **32**, 1049 (1985).
[26] P. Van Isacker, Phys. Rev. Lett. **83**, 4269 (1999).
[27] J. A. Cizewski, R. F. Casten, G. J. Smith, M. L. Stelts, W. R. Kane, H. G. Borner, and W. F. Davidson, Phys. Rev. Lett. **40**, 167 (1978).
[28] M. K. Harder, K. T. Tang, and P. Van Isacker, Phys. Lett. B **405**, 25 (1997).
[29] S. L. King *et al.*, Phys. Lett. B **443**, 82 (1998).
[30] E. A. McCutchan, R. F. Casten, and N. V. Zamfir, Phys. Rev. C **71**, 061301(R) (2005).
[31] F. Pan and J. Draayer, Phys. Lett. B **442**, 7 (1998).
[32] M. Jafarizadeh, A. J. Majarshin, N. Fouladi, and M. Ghapanvari, J. Phys. G: Nucl. Part. Phys. **43**, 95108 (2016).
[33] A. Jalili Majarshin, M. A. Jafarizadeh, and H. Sabri, Eur. Phys. J. Plus **132**, 418 (2017).
[34] A. Jalili Majarshin, Eur. Phys. J. A **54**, 11 (2018).
[35] F. Pan and J. P. Draayer, Nucl. Phys. A **636**, 156 (1998).
[36] M. Gaudin, J. Phys. **37**, 1087 (1976).
[37] J. E. García-Ramos and K. Heyde, Nucl. Phys. A **825**, 39 (2009).
[38] H. Lehmann and J. Jolie, Nucl. Phys. A **588**, 623 (1995).
[39] H. Lehmann, J. Jolie, C. De Coster, B. Decroix, K. Heyde, and J. Wood, Nucl. Phys. A **621**, 767 (1997).
[40] B. Singh, Nucl. Data Sheets **107**, 1531 (2006).
[41] K. Nomura *et al.*, Phys. Rev. C **83**, 014309 (2011).
[42] K. Nomura *et al.*, Phys. Rev. C **84**, 054316 (2011).
[43] R. F. Casten and J. A. Cizewski, Nucl. Phys. A **309**, 477 (1978).
[44] A. N. Andreyev *et al.*, Nature (London) **405**, 430 (2005).
[45] R. Gilmore, J. Math. Phys. **20**, 891 (1979).
[46] J. N. Ginocchio and M. W. Kirson, Phys. Rev. Lett. **44**, 1744 (1980).
[47] A. E. L. Dieperink, O. Scholten, and F. Iachello, Phys. Rev. Lett. **44**, 1747 (1980).
[48] P. Van Isacker and J. Q. Chen, Phys. Rev. C **24**, 684 (1981).
[49] K. Nomura, T. Otsuka, and P. Van Isacker, J. Phys. G: Nucl. Part. **43**, 024008 (2016).
[50] Live chart of Nuclides, Nuclear Structure and Decay Data (IAEA Nuclear Data Section), http://www-nds.iaea.org/relnsd/vcharthtml/VChartHTML.html
[51] C. Y. Wu *et al.*, Nucl. Phys. A **607**, 178 (1996).